# SHAPE AND SIZE ANALYSIS OF CORN PLANT CANOPIES FOR PLANT POPULATION AND SPACING SENSING

D. S. Shrestha, B. L. Steward

**ABSTRACT.** *An effective corn plant population and spacing sensing system may provide a key layer of field variability information useful for crop management. An algorithm was developed to count corn plants and to estimate plant location and intra−row spacing in segmented images of 6.1−m (20−ft) long row sections. Images were scanned to detect and determine the boundaries of top projected corn plant canopy objects using a chain code methodology. Plant objects were fused together based on a multi−step process that took into account the spatial structure of the crop row. Position, roundness, and area of plant canopies were used to distinguish between corn plants and weeds. Estimates of plant counts in row sections were compared with manual counts across three growth stages, three populations, and three tillage treatments. Overall, the system estimated the number of plants with an RMSE of 1.49 plants per row section, which corresponds to 6.2% RMSE or 3210 plants/ha (1300 plants/acre). No evidence of significant differences in mean plant spacing estimates was detected although significant, albeit small, increases in spacing variance were detected. These results demonstrate the importance of canopy shape and size analysis in the implementation of a machine vision plant population and intra−row spacing sensing system.*

***Keywords.*** *Precision agriculture, Machine vision, Image processing, Crop canopy, Sensing system, Freeman chain code.*

Recent studies have shown that plant population and spacing variability have an important effect on corn yield. Doerge et al. (2002) reported that every 25−mm (1−in.) reduction in corn plant spacing standard deviation resulted in yield increases of about 0.21 Mg/ha (3.1 bu/acre). Nafziger (1996) found that the corn plants on either side of a missing plant compensated for only 47% of the reduced yield in fields with lower population, and 19% in fields with higher population, hence decreasing crop yield.

Measurement and management of in−field plant population and spacing variability is one example of the use of precision agriculture (PA). PA is a management strategy that uses information technologies to bring data from multiple sources to bear on decisions associated with agricultural production (NRC, 1997; Robert, 2002). Documentation and increased awareness of in−field variability are important outcomes from the introduction and use of PA methodologies. Yield monitors have clearly documented spatial variation in yield (Colvin et al., 1997). In addition, the existence of variability in topography, soil characteristics, water availability, and crop growth is well known. Nevertheless, a fundamental difficulty that hinders further development and application of PA has been the development of sensors for economically measuring and characterizing in−field variability beyond that of yield.

Because of this gap, many investigations into sensing technologies for measuring field scale variability in several crop production parameters have been pursued. Yield sensors for major crops are approaching maturity and are commercially available (Zhang et al., 2002). Sensors have been developed for measuring soil properties such as soil organic matter and moisture content (Hummel et al., 2001), electrical conductivity (Lund et al., 2000), and nutrients (Birrell and Hummel, 2000). Sensors have also been developed to measure plant parameters such as at−harvest corn population (Birrell and Sudduth, 1995), nitrogen status (Goel et al., 2003), and leaf area index (Johnson et al., 2003). While not yet deployed on a field scale, image−based crop growth measurement has been shown to be effective in measuring and modeling crop plant growth in laboratory or greenhouse applications (Tarbell and Reid, 1991; Van Henten and Bontsema, 1995). Machine vision−based algorithms have been developed to estimate several crop and field parameters such as weed infestations (El−Faki et al., 2000; Tang et al., 2000), plant shape and size (Nishiwaki et al., 2001), plant population (Shrestha and Steward, 2003), and plant height (Shrestha et al., 2002).

Specifically in the area of corn population sensing, Birrell and Sudduth (1995) showed that a combine mounted mechanical sensor was an excellent estimator of hand counted population at harvest (Sudduth et al., 2000). Plattner and Hummel (1996) developed another corn population sensor using optical sensors at harvest. Shrestha and Steward (2003) demonstrated that machine vision could be effective in locating corn plants and measuring interplant spacing from

Article was submitted for review in May 2004; approved for publication by the Information & Electrical Technologies Division of ASAE in October 2004.

This journal paper of the Iowa Agriculture and Home Economics Experiment Station, Ames, Iowa, Project No. 3612, was supported by Hatch Act and State of Iowa funds. Additional research support was provided by the Iowa State University Center for Advanced Technology Development.

The use of trade names is only meant to provide specific information to the reader and does not constitute endorsement by Iowa State University.

The authors are **Dev Sagar Shrestha, ASAE Member Engineer,** Assistant Professor, Biological and Agricultural Engineering Department, University of Idaho, Moscow, Idaho; and **Brian L. Steward, ASAE Member Engineer,** Assistant Professor, Department of Agricultural and Biosystems Engineering, Iowa State University, Ames, Iowa. **Corresponding author:** Brian L. Steward, Iowa State University, 206 Davidson Hall, Ames, IA 50011; phone: 515−294−1452; fax: 515−294−2255; e−mail: bsteward@iastate.edu.

  ISSN 0883−8542 

videos of crop rows. In this earlier work, a manually selected threshold was used to classify plant and background regions and no attempt was made to distinguish corn plants from weed plants.

Advances in digital video technology have opened up possibilities of using video sensors in real−time field application for the economical acquisition of data not possible until recently. These advances include the development and adoption of the IEEE 1394 serial communications standard (IEEE, 1995) as a means for transmitting video signal from a camera to a computer. Component−based development of software promotes reuse of software objects and standard interfaces between input devices like video cameras and computers (Stevens and Pooley, 2000). Low−cost, high−speed computers have opened the way for real−time video processing (Francois and Medioni, 2001).

Often an important image−processing step in machine vision−based field information acquisition systems has been the analysis of plant leaf or canopy shape in field images. One use of the information derived from such analyses has been classifying weed and crop plants for selective or variable rate application systems (Tian et al. 1997; Lee et al., 1999). In other work, shape information has been integrated with other information such as color, shape, and planting geometry for plant classification (Tillett et al., 2001; Astrand and Baerveldt, 2002). In addition, plant features from shape analysis have been used to navigate a vehicle and generate a local map for chemical treatment (Sanchiz et al., 1996).

Shape analysis of early growth stage corn plant canopies presents challenges because (a) a variety of plant sizes exist due to differences in time of emergence, (b) the top projected view of the canopy can have substantial variation in size and shape depending on leaf orientation, (c) weeds can exist in the crop row requiring classification of corn plants and weeds, and (d) substantial variation in corn plant spacing can exist. For corn plants, the row structure can be used to classify off−row plants, but the variability in intra−row plant spacing limits the potential of using this information for estimating the next plant along the row. Despite these challenges, Shrestha and Steward (2003) showed that machine vision has good potential for sensing corn plant population and intra−row spacing. Plants were identified through the use of features of image rows, which were perpendicular to the crop row without analyzing individual plant shape.

The goal of this research was to investigate the effect of including plant canopy shape and size information on the accuracy of plant population and spacing estimates. The objectives of this research were (1) to develop a canopy shape and size analysis technique for singulating corn plants and classifying corn and weed plants within corn row sections, and (2) to analyze the accuracy of this algorithm in estimating the number of corn plants, plant location, and intra−row corn plant spacing in experimental row sections.

## Materials and Methods

Video of corn rows was collected in the field. Video frames corresponding to 6.1−m (20−ft) long row sections were mosaicked into composite images and segmented into plant and background. A spatial analysis algorithm was developed and applied, and its performance was analyzed.

### Video Collection

Corn row video was collected at the Iowa State University Agronomy and Agricultural Engineering Research Center (Boone, Iowa) during the summers of 2001 and 2002. A digital camcorder (DCR−TRV900, Sony USA, New York, N.Y.) was mounted on a utility vehicle (Gator, John Deere, Moline, Ill.) 0.60 m (24 in.) above the ground with a 0.30− × 0.40−m (12− × 16−in.) field of view. Each video frame contained 480 × 720 pixels with 24−bit color resolution. The vehicle was driven over and parallel to corn rows planted 0.76 m (30 in.) apart with the camera directly over the plants at the speed of about 3.6 km/h (2.0 miles/h). The shutter speed was 1/1000 s; frames were captured in progressive scan mode; other camera settings were set to be automatically adjusted. In the field, the video stream was recorded on a miniDV tape (JCV, Wayne, N.J.).

In the row sections, corn plants were counted manually to compare with automated counted results. The plant stem location from the beginning of each row section was manually measured to the nearest 12.7 mm (0.5 in.) and recorded. A steel measuring tape was laid out along the corn row direction, and plant location relative to the start of the row section was recorded. A total of 221 sections were measured manually. The algorithm estimated each plant location in terms of pixel coordinates from the top left corner of the first image of the video sequence for a corn row section.

### Experimental Design

The effects of three factors on counting performance were investigated. These factors were: 1) tillage, 2) growth stage, and 3) plant population. Three tillage systems were investigated: “till plant” which did not have tillage prior to planting, “plow” for which a moldboard plow was used resulting in a minimum amount of crop residue on the soil surface, and “spring disk” for which spring tillage was done using a disk or cultivator. Video was collected as the plants varied in growth stages from V3 to V8 (Ritchie et al., 1993). Plant growth stages were classified into three levels, namely V3−V4 stages, V5−V6 stages, and V7−V8 stages, to account for the existing variability in growth stages among the plants at the time of data collection. The three levels of population were 39,500, 54,000, and 74,000 plants/ha (16,000, 22,000, and 30,000 plant/acre). The experiment was designed for full factorial interaction resulting in 27 different treatment combinations. After data collection, some video segments contained saturated images and were excluded from further analysis. This led to an unbalanced dataset with the number of samples per treatment combination ranging from 7 to 28.

### Video Frame Sequencing and Segmentation

Video was acquired by a personal computer (Optiplex GX 300, Dell, Round Rock, Tex.) through an IEEE 1394 serial port using custom written software using Visual C++ (Microsoft, Redmond, Wash.). The software extracted video frames and sequenced those frames. Frame sequencing is the process of determining the amount of spatial overlap in succeeding video frames through the identification and matching of common scene points in two frames. This step was necessary to discard duplicate information and prevent multiple counting of corn plants and was accomplished with an area correspondence algorithm developed by Shrestha and Steward (2003). Composite images for each row section were

generated and segmented for vegetation using the truncated ellipsoidal method (Shrestha et al., 2001). Spatial analysis was then performed on these binary composite images.

## Spatial Analysis

A chain−code−based spatial analysis algorithm performed plant object labeling and representation in the segmented image. Holes inside a chain code of an object were detected, and neighboring objects were fused together through a multi−step process. Finally, the plant objects were classified into weeds and corn plants, and corn plant canopy center locations were estimated.

### *Plant Object Labeling and Representation*

Segmentation produced a binary image consisting of segmented plant objects and background with a pixel−by−pixel segmentation process, which had a goal of minimizing computation. Therefore, segmented images tended to consist of clusters of plant pixels, which corresponded to actual plant objects in the field of view as well as pixels segmented as plant pixels due to segmentation noise.

The plant object labeling procedure started by scanning from the upper left hand corner of the binary composite image from left to right until a plant pixel was encountered. Upon discovery of the plant pixel, the eight−neighbor chain code (Freeman, 1961) was calculated for the object using a standard algorithm (Parker, 1994). Then the chain code was translated into actual image coordinates and stored in a data structure called a chain code table in which individual elements were structures containing the object chain code, estimated object center coordinates, object area, and coordinates of the vertices of the rectangle enclosing the object. Image coordinates of the object boundary were stored instead of the object chain code to minimize future computation.

The chain code algorithm required that the chain always start from a local upper left pixel of an object. Thus upon detection of a plant pixel, two conditions had to be satisfied for it to be the starting point of the chain code of a new object: 1) the pixel must be a local upper left corner (fig. 1), and 2) it could not be part of a previously detected chain. Mathematically, the first condition was satisfied if:

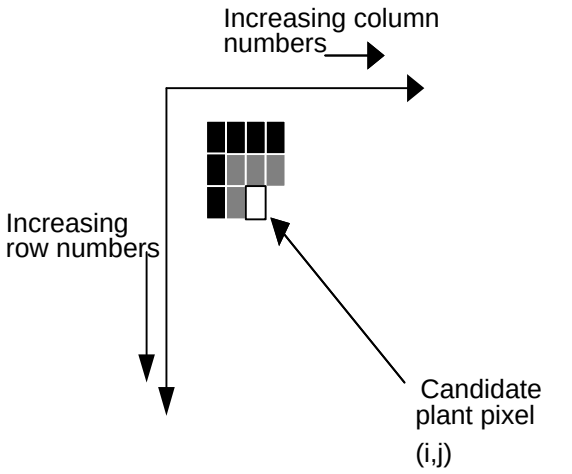


**Figure 1. Chain codes were always started from the upper left corner of objects. The algorithm determined if a detected plant pixel was at a local upper left corner of an object using the criteria given by equation 1.**

$$P_{i,j-1} + P_{i-1,j-1} + P_{i-1,j} + P_{i-1,j+1} = 0 \quad (1)$$

where i and j are the row and column coordinates of the candidate plant pixel ($P_{i,j} = 1$), which means it could not be connected to any plant pixels to its left, above, upper left, or upper right.

After detecting the first object, subsequently detected plant pixels that satisfied the first condition also had to satisfy the second condition since an object can have more than one pixel satisfying the first condition (fig. 2). Checking if the candidate pixel was a part of any of the previously detected object chain codes was unnecessary. To make the search process more efficient, an index of the chain codes, which contained just the chain codes of objects with ending row numbers that were greater than the pixel in question was generated. This greatly reduced the number of chain codes that were searched to determine if a candidate pixel was a part of a previously detected object. In addition to the chain code, a rectangular envelope enclosing an object was determined by finding the minimum and maximum coordinates for the object rows and columns. In addition, the center of the object along both row and column directions was initially estimated to be at the center of the envelope enclosing the object.

### *Hole Detection and Noise Removal*

With the above conditions for the starting point of chain code, chain codes were drawn around interior object holes in addition to exterior object edges. Thus, holes were distinguished from objects by calculating the total number of plant pixels enclosed by each chain code. If the number of enclosed pixels was equal to the perimeter, than that chain code was classified as a hole. This criterion also classified one and two pixel wide objects as holes, but this was not of concern for this application since plants were wider objects given the spatial resolution of the sensing system. Upon detection, holes were deleted from chain code table.

In addition to the holes, very small objects were also removed from consideration as plants. Based on

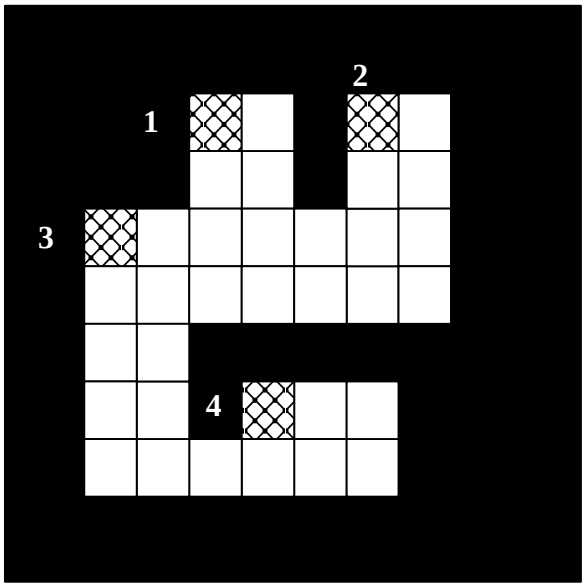


**Figure 2. Example of an object with more than one chain code starting pixel, shown as cross hatched. All of the cross hatched pixels 2−4 are also a part of the chain code starting with candidate pixel 1.**

150 manually segmented plants, the mean top projected canopy area of V3 growth stage plants was 2450 pixels, which corresponded to 1290 $mm^2$ (2.0 $in.^2$). Any object smaller than a threshold of 100 pixels was considered to be noise and was deleted from the chain code table. This number was arbitrarily chosen to be about 5% of the mean top projected plant canopy area at the V3 stage and was equivalent to 64.5 $mm^2$ (0.1 $in.^2$).

### *Object Fusion*

The plant segmentation process resulted in fragmented objects from single plants. This fragmentation has various causes. In many cases, it was due to image hot spots from specular reflections. These disconnected objects must be fused together into a complete plant object. However, the fusion algorithm must be designed so that neighboring plants are not fused together as a single plant. To avoid the fusing of neighboring plants along the crop row, the fusion process was subdivided into three steps.

In the first step, only small objects, which were fully contained within the image rows spanned by a larger object, were considered for fusion. This step was implemented to avoid unconstrained growth of objects along the crop row. The chain code table had the information about the minimum and maximum rows and object spans denoted by $R_{x1}$ and $R_{x2}$, respectively. If an object y, regardless of size and distance is completely within the row limits of another object x, then it was considered for fusion (fig. 3). Mathematically, if $R_{y1} \geq R_{x1}$ and $R_{y2} \leq R_{x2}$ then two objects were marked for fusion based on the criteria that the distance between the two object centers was less than the sum of the half diagonals of the two objects. An object's half diagonal was defined as the distance from the object center to a corner of the rectangle surrounding the object. If the small object was outside of the distance criteria, then it was deleted. The actual fusion of the object was done only at the end of comparison of all objects in the composite image. This process was based on the assumption that the plant objects were bigger than weed objects. There was potential for error if small corn plants were contained within the image rows spanned by a larger weed. However, this condition was not common in the row sections observed. After fusion, a fused object center was then calculated using the equation:

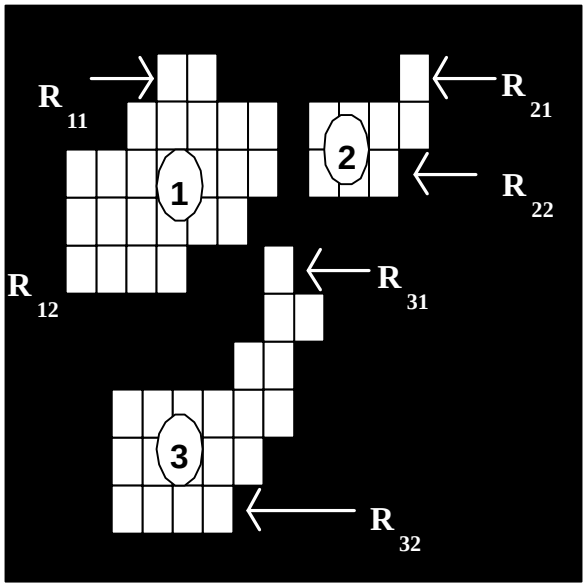


**Figure 3. In the first step of the fusion process, only objects contained within the row limits ($R_{x1}$ and $R_{x2}$) of another object are considered for fusion. Object 2, for example, is completely within the row limits of Object 1 ( $R_{21} >= R_{11}$ and $R_{22} <= R_{22}$) hence objects 1 and 2 are considered for fusion. Object 3 is not considered in this step.**

$$\mathbf{C}_{new} = \frac{A_1\mathbf{C}_1 + A_2\mathbf{C}_2}{A_1 + A_2} \quad (2)$$

where $C_1$ and $C_2$ were the row and column center coordinate vectors of the individual objects and $A_1$ and $A_2$ were the object areas in pixels. This process removed small weeds and noise pixels, which were in between the row limits of a bigger plant object. However, the small objects, which were not contained within the rows of a bigger object, were not removed in this process.

In the second step of object fusion, a straight line was fit to the fused object center locations using weighted least squares where the weights were object areas. Larger objects were given a higher weight to minimize the effect of small stray objects on the regression line. The line followed the equation:

$$y = m\,x + b \quad (3)$$

where y was the column position of the line for a given row x, and m and b were the slope and column position of the regression line at the first row, respectively. From a standard weighted least squares technique (Draper and Smith, 1998), the parameters describing the line were estimated using:

$$B = \left[X^T V X\right]^{-1} X^T V Y \quad (4)$$

where

$B = [m \quad b]^T$

$$X = \begin{bmatrix} x_1 & x_2 & \ldots & x_n \\ 1 & 1 & \ldots & 1 \end{bmatrix}^T$$

$x_i$ = the row coordinate of the estimated center of object i
V = a diagonal matrix with diagonal elements as object area

$Y = [y_1\ y_2\ \ldots\ y_n]^T$
$y_i$ = the row coordinate of the estimated center of object i
Superscript T = matrix transpose

After the line parameters m and b were estimated, a buffer region was defined on both sides of the mean row line calculated from the line parameters. The buffer was chosen to be 200 pixels [approximately 150 mm (6 in.)] on both sides of the regression line to allow for deviation in plant location from the line or for line curvature caused by driving error or other reasons. Any object that was outside of the buffer region was considered to be a weed and was deleted.

In the third step, all remaining objects were sorted based on their distance from the top of the composite image, $R_{x1}$, in figure 3. Starting with the first object and its nearest neighbor, object pairs were analyzed and fused together if they met the following criteria:

- their estimated center locations were less than 50 mm apart (Birrell and Sudduth, 1995), or
- the distance between their estimated centers was less than the sum of the two object half diagonals, and
- the sum of the canopy area of the combined objects was less than the mean canopy area of all detected objects or the smaller of two objects was only 10% of the size of the combined object.

These multiple criteria were chosen to avoid unbounded growth along the crop row. No objects were deleted in this step.

### *Object Classification*

Plant objects were classified as either weeds or corn plants using two features, roundness and area. From observations, weeds were round and small compared to corn plants, which were larger and had more complicated perimeters. The roundness feature was defined as the ratio of an object's area to its equivalent circular area, $A_{eq}$. Equivalent circular area was calculated from the equivalent radius of a circle, $R_{eq}$, with a perimeter, L, which is the length of the object's chain code. $R_{eq}$ was given by:

$$R_{eq} = \frac{L}{2\pi} + \frac{1}{2} \tag{5}$$

where the first term on the right side gives the distance from the circle center to the middle point of circumference pixel. An additional half a pixel width was added to include the additional area in the outside half of the circumference pixel. Mathematically, an object's roundness was defined as:

$$R_n = \frac{A}{\pi R_{eq}^2} \tag{6}$$

where A is the canopy area. Given this definition, roundness should be between zero and one. For circular objects, roundness will be close to one, or exceed one, due to digitization error. Objects departing from a circular shape will have lower roundness values.

Roundness values of 250 corn plants and 250 weeds were calculated from images acquired at each of three different corn plant growth stages. Normal distributions were fit to the histograms of each class and growth stage. In each case, mean corn plant roundness was significantly lower than that of weeds and the variance of each was similar in all three growth stages (table 1). Based on this analysis, a single roundness threshold of 0.2 was chosen to minimize classification error across all three growth stages.

As there was overlap in the weed and corn plant roundness distributions, a second feature, object area, was used in conjunction with roundness to classify weeds from corn plants. The area of weeds and corn plants was normally distributed, and the number and size of the weeds was assumed to vary spatially. Area had a low cross−correlation with roundness and hence was treated separately. The Otsu method (1979) was used to calculate the threshold between corn plant and weed area distribution curves. In cases where no weeds existed in a row section, the Otsu method would give an erroneous threshold value because the area feature would follow a unimodal distribution. Therefore, the ratio of "between variance" to "total variance" was used as a measure of separability for two distributions as suggested by Otsu. The separability measure ranged from 0 to 1, with a low separability indicating a unimodal distribution caused by a low number of detected weeds compared to corn plants. The threshold obtained from the Otsu method was multiplied by the separability value to obtain a modified threshold that was effective even for cases where few weeds existed. An object with a roundness value greater than 0.2 and area less than the modified threshold obtained from the Otsu method was classified as a weed and no longer considered. If the area of a remaining fused object was more than twice as big as the average plant area, it was classified as a double plant; more than thrice, a triple.

**Table 1. Second order statistics of the roundness feature of corn plants and weeds at three different corn growth stage levels.**

| Growth Stage Level | Corn Plant Roundness | | Weed Roundness | |
|---|---|---|---|---|
| | Mean | Std Deviation | Mean | Std Deviation |
| V3 – V4 | 0.15 | 0.07 | 0.30 | 0.17 |
| V5 – V6 | 0.15 | 0.08 | 0.43 | 0.19 |
| V7 –V8 | 0.06 | 0.06 | 0.31 | 0.19 |

### *Plant Center Location Estimation*

The centers of the singulated corn plants were re−estimated using the chain code boundary. Each plant center was estimated to be the location that minimized the sum of squared distances from it to all boundary coordinates. Let ($x_i$, $y_i$) be the plant boundary coordinates, where i = 1 to n. Then mathematically, if an object center is (x, y), then the sum of squared distances is given by:

$$e = \sum_{i=1}^{n} \left[ (x_i - x)^2 + (y_i - y)^2 \right] \tag{7}$$

Differentiating equation 7 with respect to x and y and then equating to zero results in:

$$\begin{bmatrix} x \\ y \end{bmatrix} = \frac{1}{n} \begin{bmatrix} \sum_{i=1}^{n} x_i \\ \sum_{i=1}^{n} y_i \end{bmatrix} \tag{8}$$

which was used as the final estimate of plant center location.

When an object was classified as a double or triple plant, the object was divided along image rows into sub−regions equal to the number of plants, and then equation 8 was applied within each sub−region to estimate the initial plant centers. The distance from each boundary pixel to each of the centers was next calculated. Each boundary pixel was then associated with the closest plant center. The plant centers were recalculated from equation 8 for each group.

## Performance Analysis

Three−way ANOVA was used to study the effects of the main factors (tillage, growth stage, and population) and their interactions on mean plant−counting error. Homogeneity of error variance across the main factor levels was tested using the modified Levene test (Conover et al., 1981). Root mean squared error (RMSE) was calculated and used to represent the standard error of the estimated plant count relative to the manual plant counts. Regression analysis was used to

evaluate overall performance of the algorithm with respect to the manual counts.

Plant locations were estimated relative to the end of the crop row section. Each manually observed plant was paired with the nearest plant detected by the algorithm. The difference in distance along the crop row was calculated and called location estimation error. Homogeneity of variance was tested using the modified Levene test.

For plant spacing estimates, the interplant distances between every detected plant pair were converted from pixels into physical units. The second order statistics of intra−row distances were estimated for both manual measurements and algorithm estimates. T−tests were used to check for differences between mean manually measured and algorithm estimated intra−row plant spacing. Homogeneity of variance was tested using the modified Levene test.

## Results and Discussion

Linear regression was used to analyze the relationship between the manual and automated plant counts in row sections. The manual plant counts in row sections varied from 13 to 38 plants, which corresponded to populations of 27,000 to 81,500 plants/ha. The linear model had a coefficient of determination ($R^2$) of 0.92 and an RMSE of 1.49 plants, which was 6.2% of the mean manual count of 24.1 counts per experimental unit (fig. 4). The estimated slope of the regression line was 1.00 with 95% confidence interval of 0.96 to 1.04. The estimated y−intercept was not significant at the 5% significance level. The residual plot did not reveal any observable changes in variance across the range of manual counts. Further analysis showed that row sections with high weed densities were those with the highest error.

### Mean Plant Count Estimation Error

The mean plant count estimation error was significantly different across tillage treatments ($F_{2,214}$ = 12.17, P < 0.0001). No evidence of significant differences across population ($F_{2,214}$ = 1.7, P = 0.19) and growth stage ($F_{2,214}$ = 2.72; P = 0.07 ) treatments was found. Therefore, the data were separated by tillage treatment, and regression analysis was performed on each subset. RMSE for the plow tillage treatments was 4.9%, for till plant it was 5.6% and for spring disk it was 7.1%. The lowest RMSE was associated with the plow tillage treatment where the weed density was low, and the highest RMSE belonged to the spring disk tillage treatment. Careful observation of data revealed that for the spring disk tillage treatment, the weed density was higher contributing to a higher error rate. The presence of smaller corn plant−sized weeds biased the plant size distribution curve, which in effect biased the Otsu threshold to be lower. The resulting lowered threshold resulted in more weeds classified as corn plants and hence reduced the average plant size statistics. This led to some large plants being counted as doubles.

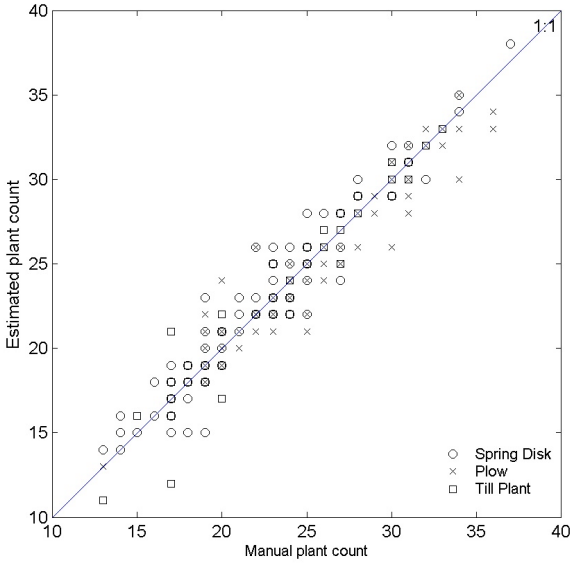


**Figure 4. Estimated machine vision plant counts vs. manual plant count data for 221 experimental units. The regression line was not significantly different from 1:1 line with $r^2$ = 0.92.**

For the spring disk tillage treatment, the algorithm overestimated the number of plants by an average of 0.3 plants per experimental unit. This difference was significantly greater than zero ($t_{84}$ = −2.48, P = 0.01). For the plow tillage treatment, the mean automated count was 0.06 plants less than the manual count and was not significantly different than 0 ($t_{63}$ = 0.31, P = 0.76). For till plant, the mean automated count was 0.5 plants less than the manual count and was significant ($t_{71}$ = 2.83, P = 0.01).

These differences in mean error were explainable based on observations of the field surface for the different tillage treatments. In particular, the amount of residue on the field surface was different for different tillage systems. For the plow tillage treatment, the field had almost no residue or weeds. There were relatively few noise pixels in the segmented images, and the variance of the corn plant size distribution was lower. These cleaner surface conditions enabled more accurate estimation of the actual plant size and better classification of small weeds from corn plants. For the till plant treatment, the field was covered with crop residue and a few weeds were visible, but there were many double plants growing close to each other. If there were many double plants in a row, the average plant area estimated by the algorithm would be biased towards a higher value. This biasing led to double plants being classified as single plants and also led to underestimation of plant counts. The opposite was true for the spring disk tillage treatment where the presence of many weeds biased the mean plant size towards lower values.

The algorithm produced images showing the estimated location of corn plants. Visual inspection revealed that the algorithm was able to effectively singulate both small and large plants. Segmentation noise was effectively removed by deleting the small objects. The object fusion algorithm was effective in grouping the fragmented parts of a whole plant (fig. 5). The algorithm was also effective in separating adjacent corn plants with leaves crossing over the same image rows provided the sum of the two plant areas were greater than the mean object canopy area. The ability of correcting segmentation error without fusing two close plants was one of the main advantages of applying plant shape analysis to group the objects over prior methods (Shrestha and Steward, 2003).

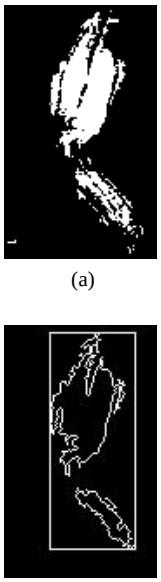

(a) (b)

**Figure 5. Example of (a) segmented corn plant, and (b) rectangle around box showing the extent of a corn plant object consisting of fused fragmented objects.**

### Plant Count Error Variance

Plant count error variance was significantly different only across growth stages ($F_{2,218}$ = 3.28; P = 0.039), and no evidence of differences across tillage treatments ($F_{2,218}$ = 2.56; P = 0.08) or population ($F_{2,218}$ = 0.67; P = 0.51) was found. In particular, the error variance for the V7−V8 growth stage level was significantly higher than the error variance for V3−V4 or V5−V6 growth stages. No evidence of differences in the error variance between V3−V4 and V5−V6 growth stages was found. These results indicate that the uncertainty of population estimates increases at later growth stages.

A minimum RMSE of 0.38 plants was found for till plant tillage treatment at V3−V4 growth stage and 54,000 plants/ha (22,000 plants/acre), which was 1.65% of the mean plant count (table 2). This result was better than that reported by Shrestha and Steward (2003) and came from the effectiveness of shape analysis code algorithm in separating two close plants (fig. 6). In general, error variance was higher for later growth stages. The emergence time for the corn plant varied,

**Table 2. RMSE of plant count estimates in row sections for different tillage, growth stage, and plant population density combinations.**

| Population (plants/ha) | Tillage | Growth Stage[a] | | |
|---|---|---|---|---|
| | | V3−V4 | V5−V6 | V7−V8 |
| 39,500 | Spring disk | 1.10 (6.2) | 1.73 (8.9) | 1.83 (8.8) |
| | Plow | –[b] | – | 2.56 (13.1) |
| | Till plant | – | – | 1.89 (10.2) |
| 54,000 | Spring disk | 1.36 (6.4) | 1.65 (7.7) | – |
| | Plow | 0.76 (3.3) | 1.35 (6.1) | – |
| | Till plant | 0.38 (1.7) | 1.46 (6.4) | 1.71 (7.2) |
| 74,000 | Spring disk | 1.37 (4.5) | – | – |
| | Plow | 1.41 (4.6) | 1.65 (5.6) | – |
| | Till plant | 0.68 (2.3) | – | – |

[a] Numbers in parenthesis are RMSE as a percentage of mean plant count for a particular treatment combination.
[b] Data not available.

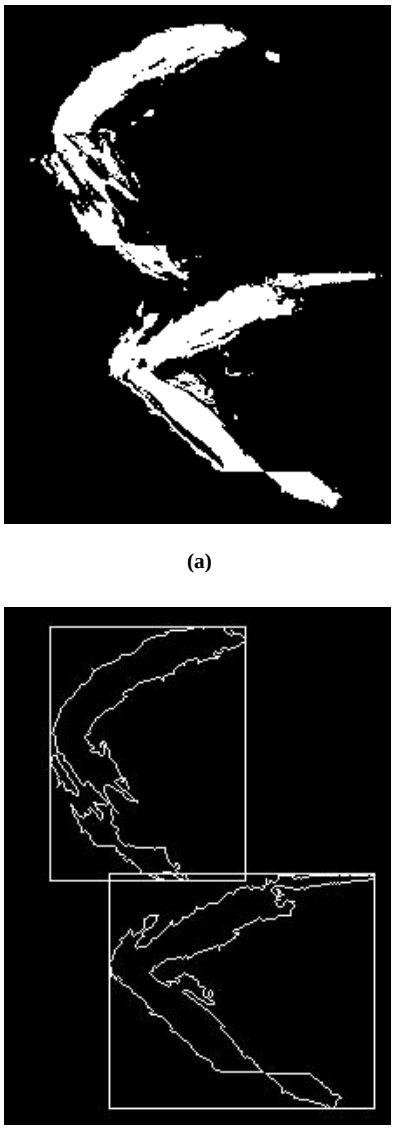

(a) (b)

**Figure 6. Example of two plant objects (a) that were not fused (b) because the sum of two objects would have been greater than average object size and the size of each individual object is comparable.**

and the corn plants that emerged later tended to have smaller size at initial stages than the plants that emerged earlier. The difference in size increased with growth stage. As the variability in corn plant canopy area increased, it was more difficult to differentiate between weeds and corn plants. Weed density varied between different experimental units. However, because of the greater variation in plant size, the presence or absence of weeds affected population estimation performance more at higher growth stage.

### Plant Location Estimation Accuracy

No significant effect on mean plant location estimation error by any of the factors was observed. This error was 0.6 mm (0.02 in.), which was not significantly different than zero ($t_{3243}$ = 0.52, P = 0.60), and the standard deviation of the location estimation error was 63.5 mm (2.5 in.). The magnitude of the estimation error variance was due in part to the analysis method. Each detected plant was matched with

the nearest manually measured plant location. The plant center location estimates were reasonable but did not guarantee that the calculated center was within the plant boundary. In addition, when a manually recorded plant was not detected by the algorithm, the nearest detected plant was assumed to be the corresponding plant, thus substantially increasing the spacing error (fig. 7). However, misclassified weeds had no effect on location measurement accuracy, since weeds were not counted during manual measurements.

The variance in the location estimation error was significantly different across growth stages ($F_{3238,2}$ = 4.18; P = 0.015), but no evidence of a population effect was found. Error variance increased with increasing growth stages because plant center locations were manually measured differently than they were estimated by the algorithm. Plant center locations were manually measured to the position of plant stem, but the algorithm estimated plant center location was the point that minimized the sum of distance squared from the plant canopy boundary. When the plants were smaller in size, their leaves were smaller and more symmetrically spread out from the stem which led to lower variance in the location error. At later growth stages, however, because of the larger, more asymmetrical canopy development, the leaf area centers were more likely to deviate further from the plant stem position, leading to an increased error variance.

### Plant Spacing Estimation Accuracy

No evidence of significant differences between the mean measured and estimated interplant spacing was found across combinations of all tillage treatments and two population treatments (table 3). However, the modified Levene test for equal variance on manual and estimated plant spacing standard deviation showed that the estimated variance was treatments (table 3). However, the modified Levene test for equal variance on manual and estimated plant spacing standard deviation showed that the estimated variance was

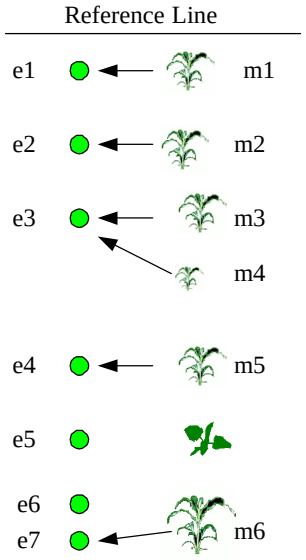


**Figure 7. Location measurements relative to the start of a row section were compared pair−wise. Each manually observed plant was paired with the estimated located nearest to it. Plants m1, m2, m3, m4, m5, and m6 were matched with plants e1, e2, e3, e3, e4, and e7, respectively. Plant m4 was not detected and hence erroneously matched with e3.**

**Table 3. Intra−row spacing for different plant population and tillage treatments.**

| Population (plants/ha) | Tillage | Intra−Row Spacing (mm) | |
|---|---|---|---|
| | | Measured | Estimated |
| 39,500 | Spring disk | 318 (246)[a] | 323 (255) |
| | Plow | 328 (264) | 325 (270) |
| | Till plant | 371 (290) | 371 (306) |
| 54,000 | Spring disk | 277 (198) | 277 (203) |
| | Plow | 267 (173) | 267 (183) |
| | Till plant | 279 (216) | 279 (221) |

[a] Numbers in the parenthesis represent standard deviation.

significantly higher than the measured plant spacing standard deviation (P < 0.001 for all cases). Increases in standard deviation ranged from 4.8 to 16.2 mm (0.18 to 0.64 in.) across all treatment combinations. The larger variance was primarily due to the algorithm's method of estimating plant center locations.

## Conclusion

An image analysis technique was developed to extract shape and size features from top projected plant canopies. This research demonstrated that:

- Area and roundness features from top projected plant canopies can be used to classify weeds and corn plants resulting in increased accuracy of population and spacing estimates. Mean roundness ranged from 0.06 to 0.15 for corn plants and 0.30 to 0.43 for weeds for set of plants analyzed.
- Use of plant canopy shape analysis improves population estimates through fusing fragmented plant objects and distinguishing between corn and weed plants. The overall algorithm estimated the number of plants in 6.1−m row sections with an overall RMSE of 1.49 plants. A tillage treatment effect was detected on mean plant count estimation error, while growth stage affected plant location error variance because of the presence of larger weeds and greater plant size variability.

## References


Astrand, B., and A. Baerveldt. 2002. An agricultural mobile robot with vision−based perception for mechanical weed control. *Autonomous Robots* 13(1): 21−35.

Birrell, S. J., and J. W. Hummel. 2000. Membrane selection and ISFET configuration evaluation for soil nitrate sensing. *Transactions of the ASAE* 43(2): 197−206.

Birrell, S. J., and K. A. Sudduth. 1995. Corn population sensor for precision farming. ASAE Paper No. 951334. St. Joseph, Mich.: ASAE.

Colvin, T. S., D. B Jaynes, D. L. Karlen, D. A. Laird, and J. R. Ambuel. 1997. Yield variability within a central Iowa field. *Transaction of the ASAE* 40(4): 883−889.

Conover, W. J., M. E. Johnson, and M. M. Johnson. 1981. A comparative study of tests for homogeneity of variances, with applications to the outer continental shelf bidding data. *Technometrics* 23(4): 351–361.

Doerge, T., T. Hall, and D. Gardner. 2002. New research confirms benefits of improved plant spacing in corn. Pioneer Hi−Bred International, Inc. *Crop Insights* 12(2): 1−5.

Draper, N. R., and H. Smith. 1998. *Applied Regression Analysis*, 3rd Ed. New York: John Wiley.

El−Faki, M. S., N. Zhang, and D. E. Peterson. 2000. Weed detection using color machine vision. *Transactions of the ASAE* 43(6): 1969−1978.

Francois, A. R. J., and G. G. Medioni. 2001. A modular software architecture for real−time video processing. *IEEE 2nd International Workshop on Computer Vision Systems (ICVS'01), International Conference on Computer Vision (ICCV).* Vancouver, BC: IEEE.

Freeman, H. 1961. On the encoding of arbitrary geometric configurations. *IEEE Transactions On Electronics and Computers* EC−10: 260−268.

Goel, P. K., S. O. Prasher, R. M. Patel, J. A. Landry, R. B. Bonnell, and A. A. Viau. 2003. Classification of hyperspectral data by decision trees and artificial neural networks to identify weed stress and nitrogen status of corn. *Computers and Electronics in Agriculture* 39(2): 67−93.

Hummel, J. W., K. A. Sudduth, and S. E. Hollinger. 2001. Soil moisture and organic matter prediction of surface and subsurface soils using an NIR soil sensor. *Computers and Electronics in Agriculture* 32(2): 149−165.

IEEE. 1995. IEEE Standard for a High Performance Serial Bus, IEEE Standard 1394−1995. New York: IEEE.

Johnson, L. F., D. E. Roczen, S. K. Youkhana, R. R. Nemani, and D. F. Bosch. 2003. Mapping vineyard leaf area with multispectral satellite imagery. *Computers and Electronics in Agriculture* 38(1): 33−44.

Lee, W. S., D. C. Slaughter, and D. K. Giles. 1999. Robotic weed control system for tomatoes. *Precision Agriculture* 1(1): 95–113.

Lund, E. D., C. D. Christy, and P. E. Drummond. 2000. Using yield and soil electrical conductivity (EC) maps to derive crop production performance information. In *Proc. Fifth International Conference on Precision Agriculture*, eds. P. C. Robert, R. H. Rust, and W. E. Larson. Madison, Wis.: ASA, CSSA, and SSSA.

Nafziger, E. D. 1996. Effects of missing and two−plant hills on corn grain yield. *J. of Production Agriculture* 9(2): 238−240.

National Research Council. 1997. *Geospatial and Information Technologies in Crop Management.* Washington, D.C.: National Academy Press.

Nishiwaki, K., T. Togashi, K. Amaha, and K. Matsuo. 2001. Estimate crop position using template matching in rice production. ASAE Paper No. 013103. St. Joseph, Mich.: ASAE.

Otsu, N. 1979. A threshold selection method from gray − level histograms. *IEEE Transactions on Systems, Man, and Cybernetics* 9(1): 62−66.

Parker, J. R. 1994. *Practical Computer Vision Using C*. New York: John Wiley.

Plattner, C. E., and J. W. Hummel. 1996. Corn plant population sensor for precision agriculture. In *Proc. 3rd International Conference on Precision Agriculture*, eds. P. C. Robert, R. H. Rust, and W. E. Larson, 785–794. Madison, Wis.: ASA, CSSA, and SSSA.

Ritchie, S. W., J. J. Hanway, and G. O. Benson. 1993. How a corn plant develops. Iowa State University Cooperative Extension Service Special Report No. 48. Ames, Iowa: ISU.

Robert, P. C. 2002. Precision agriculture: a challenge for crop nutrition management. *Plant and Soil* 247(1): 143−149.

Sanchiz, J. M., F. Pla, J. A. Marchant, and R. Brivot. 1996. Structure from motion techniques applied to crop field mapping. *Image and Vision Computing* 14(5): 353−363.

Shrestha, D. S., and B. L. Steward. 2003. Automatic corn plant population measurement using machine vision. *Transactions of the ASAE* 46(2): 559−565.

Shrestha, D. S., B. L. Steward, S. J. Birrell, and T. C. Kaspar. 2002. Corn plant height estimation using two sensing systems. ASAE Paper No. 021197. St. Joseph, Mich.: ASAE.

Shrestha, D. S., B. Steward, and E. Bartlett. 2001. Segmentation of plant from background using neural network approach. In *Intelligent Engineering Systems through Artificial Neural Networks: Proc. Artificial Neural Networks in Engineering (ANNIE) International Conference*, 11: 903–908. New York: ASME Press.

Stevens, P., and R. Pooley. 2000. *Using UML*. Harlow, England: Addison−Wesley.

Sudduth, K. A., S. J. Birrell, and M. J. Krumpelman. 2000. Field evaluation of a corn population. In *Proc. 5th International Conference on Precision Agriculture*, eds. P. C. Robert, R. H. Rust, and W. E. Larson. Madison, Wis.: ASA, CSSA, and SSSA.

Tang, L., L. Tian, and B. L. Steward. 2000. Color image segmentation with genetic algorithm for in field weed sensing. *Transactions of the ASAE* 43(4): 1019−1027.

Tarbell, K. A., and J. F. Reid. 1991. A computer vision system for characterizing corn growth and development. *Transactions of the ASAE* 34(5): 2245−2255.

Tian, L., D. C. Slaughter, and R. F. Norris. 1997. Outdoor field machine vision identification of tomato seedlings for automated weed control. *Transaction of ASAE* 40(6): 1761−1768.

Tillett, N., T. Hague, and S. J. Miles. 2001. A field assessment of a potential method for weed and crop mapping on the basis of crop planting geometry. *Computers and Electronics in Agriculture* 32(3): 229−246.

Van Henten, E. J., and J. Bontsema. 1995. Non−destructive crop measurements by image processing for crop growth control. *J. Agric. Eng. Res.* 61: 97−105.

Zhang, N. Q., M. H. Wang, and N. Wang. 2002. Precision agriculture − a worldwide overview. *Computers and Electronics in Agriculture* 36(2−3): 113−132.